Automated Detection of Breast Contour in 3D Images of the Female Torso

Lijuan ZHAO[1], Shishir K. SHAH[1], Gregory P. REECE[2], Melissa A. CROSBY[2], Michelle C. FINGERET[2,3], and Fatima A. MERCHANT*[1,4]
[1]Department of Computer Science, University of Houston, Houston (TX), USA;
[2]Department of Plastic Surgery, The University of Texas MD Anderson Cancer Center, Houston (TX), USA;
[3]Department of Behavioral Science, The University of Texas MD Anderson Cancer Center, Houston (TX), USA;
[4]Department of Engineering Technology, University of Houston, Houston (TX), USA

http://dx.doi.org/10.15221/13.273

Abstract

Stereophotogrammetry is finding increasing use in plastic surgery, both for breast reconstruction after oncological procedures and cosmetic augmentation/reduction. The ability to visualize and quantify morphological features of the breast facilitates pre-operative planning and post-operative outcome assessment. Breast contour is an important attribute for quantitative assessment of breast aesthetics. Based on the detected breast contour, relevant morphological measures such as breast size, shape, symmetry, volume and ptosis can be determined. In this study we present an approach for the automatic contour detection of the lower breast in three-dimensional (3D) images. Our approach employs surface curvature analysis. We first identify the points with the lowest Gaussian curvature within the one-ring neighborhood on the surface mesh, and then apply the random sample consensus (RANSAC) algorithm to non-deterministically estimate the lower breast contour from the set of low curvature points.

Keywords: 3D image, breast contour detection, Gaussian curvature, RANSAC algorithm

1. Introduction

Breast reconstruction is an important surgical component for many women undergoing breast cancer treatment [1]. Breast cancer remains one of the most common malignancies in women and is one of the leading causes of cancer-related mortality. Despite the current emphasis on breast conservation, mastectomy rates remain at 30%. Mastectomy is often associated with significant psychological stress due to distorted body image. Predominantly, the purpose of breast reconstruction is to restore the breasts and correct the deformations, thereby facilitating improvement in psychosocial well-being and quality of life in breast cancer survivors [2].

Stereophotogrammetry is finding increasing use in quantifying breast morphology, e.g. breast shape, symmetry, and volume [3-5]. Quantitative analysis of the patient's breast shape (morphometry) is critical for pre-operative planning and post-operative assessment of outcomes in breast reconstruction [1]. Breast contour is an important attribute to evaluate the aesthetic outcomes of breast cancer treatments. The detected breast contour enables computation of morphological measures such as breast size, shape, symmetry, volume and ptosis.

Previous studies on breast contour detection have been performed on two-dimensional (2D) images and 2D range images encoding depth. Cardoso et al. [6, 7] described an automatic method for the detection of the lower breast contour in 2D images. The external endpoint of the breast contour was detected by defining it as the highest point of the trunk contour, which may be searched among the strongest lines of gradient with approximate vertical direction. The internal endpoint was estimated simply as the mid-point between the two external endpoints. After modeling the image as a weighted graph based on the gradient values and prior shape information, the breast contour was computed as the solution to the shortest-path problem between the internal and external endpoints. In subsequent studies [8, 9], this approach was extended to perform tracing of the lower breast contour in depth-map images. Both 2D images and depth-map images cannot capture the overlapped regions, e.g. the underside regions of the breasts with high ptosis degree. They detected a 2D breast boundary, rather than the 3D breast contour in the surface scan. Lee et al. [10, 11] introduced a measure of lower breast contour in 2D images which enforced a mathematical shape constraint based on the catenary curve. First, they used a catenary curve to approximate the overall breast contour, and extracted a shape

*fmerchan@central.uh.edu; +1- 713- 743- 8292; www.tech.uh.edu/faculty/merchant/

parameter, which is a measure of the breast contour representing the outlining catenary curve. The catenary-based shape measure was used by Lee et al. to evaluate the upper and lower breast contour in 3D images of patients [12]. The outlines of the upper and lower breast were first obtained from coronal sectional views that were created from multiple parallel planes to the chest wall, spaced at about $1cm$ intervals starting at the anterior most part of the breast. Then the breast contour was extracted by fitting catenary curves to the resulting outline in each sectional view. Although this method used 3D images as input, the obtained breast contours are curves in 2D planes, and do not directly mirror the 3D breast contours.

In this study, we describe a curvature-based method to automatically detect the contour of the lower breast in 3D surface scans. To the best of our knowledge, this is the first approach described so far to directly compute the breast contour on the 3D surface mesh.

2. Method

2.1. Gaussian curvature analysis

Curvature is defined as the amount that a surface deviates from being flat. At each point p of a 3D surface one may find a normal plane, which contains the normal vector of the point p. The intersection of the normal plane and the 3D surface is a plane curve. The plane curves from different normal planes at point p will generate different curvatures. The principal curvatures, k_{max} and k_{min}, are the maximum and minimum values of the curvatures at p. Gaussian curvature k is the product $k_{max}k_{min}$ of two principle curvatures. In a 3D surface, the regions with $k > 0$ are elliptic, those with $k < 0$ are hyperbolic, and those with $k = 0$ are either planar or cylindrical.

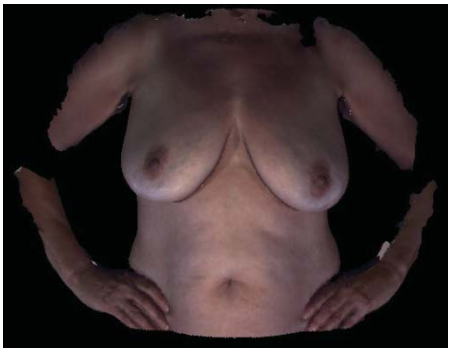

Fig. 1. Representative 3D image of the female torso. The texture image is overlaid on the surface mesh.

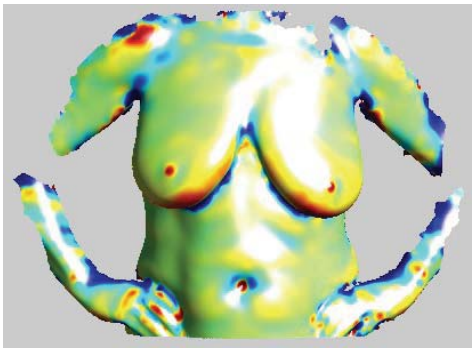

Fig. 2. Color-mapped Gaussian curvatures of 3D surface scan.

To calculate the Gaussian curvature on 3D surface mesh, we used a toolbox developed by Gabriel Peyre [13] based on the algorithms proposed by Cohen-Steiner et al. [14, 15]. The curvature tensor for each vertex was estimated using the following expression [15]:

$$T(v) = \frac{1}{|B|} \sum_{edges\ e} \beta(e)|e \cap B|\, \bar{e}\bar{e}^t \qquad (1)$$

where v is an arbitrary vertex on the 3D mesh, $|B|$ is the surface area around v over which the curvature tensor is estimated, $\beta(e)$ is the signed angle between the normal vectors to the two oriented triangles incident to edge e (positive if convex, negative if concave), $|e \cap B|$ is the length of $e \cap B$ (always between 0 and $|e|$), and $\bar{e}$ is a unit vector in the same direction as e. The tensor is evaluated by approximating the neighborhood B as the geodesic disk around this vertex. D_{max} and D_{min} are the two eigenvalues calculated from the tensor vector and provide estimates of principal curvatures at v. We employed pseudo-color visualization method for viewing the Gaussian curvature of the 3D mesh. Fig. 1 presents a representative 3D image of the torso, and the color-mapped Gaussian curvature for the torso is presented in Fig. 2. In Fig. 2, the color red represents elliptic regions, blue represents hyperbolic regions, and green represents regions near planar or cylindrical.

2.2. Determination of concave points on the surface mesh

On a 3D surface, negative curvature values correspond to concave regions, and can thus be used to identify the inward curving crease below the breast that delineates the lower breast contour. Initially,

we determine a set of concave points sCP that exhibit the lowest curvature values on 3D surface scan. This is accomplished by identifying for each vertex v, all points within its one-ring neighborhood on the surface mesh that exhibit the lowest Gaussian curvature. The one-ring neighborhood of a vertex v is the set of vertices, which are connected to v by an edge. This set of points, sCP, includes not only the points lying along the breast contour, but also randomly scattered points on the torso that represent isolated incidences of low curvature values due to mesh undulation (noise).

2.3. Lower breast contour determination

In order to differentiate points on the lower breast contour from the noisy low curvature points, we apply the RANSAC algorithm [16] to non-deterministically estimate the points lying on the breast contour from the set of low curvature points sCP.

This algorithm is applicable to both breasts but for simplicity, is discussed here in terms of the right breast. First, we find the right breast peak point (point with largest z-coordinate) in the right half part of the torso. Next, we compute the Euclidean distance between each point in sCP and the peak point. The sCP points at distances $< 20\,mm$ and $> 160\,mm$ from the peak point are removed from consideration, as at these distances the points are either too close or farther away from the peak point, and thus highly unlikely to fall along the breast contour. In addition, we also sort and keep only the sCP points that fall below a horizontal line which is $40\,mm$ above the peak point (as identified from the y-coordinate) since we need to detect the lower breast contour. We add a margin of $40\,mm$ above the peak point since the peak point would be very low for the breast with high ptosis (Fig. 3.).

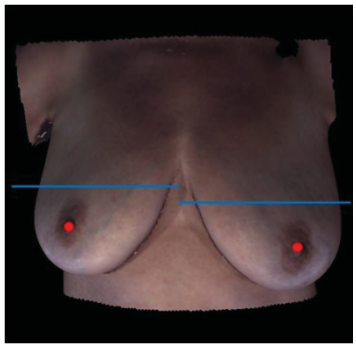

Fig. 3. Peak points (red) and cut-off lines (blue, 40 mm above the peak points) displayed on the 3D surface scan.

The RANSAC algorithm is implemented to detect the contour points as follows. In each iteration, we randomly select a set of few points p_1 from the sCP and then apply cubic spline curve fitting to the points in p_1. The distance of each remaining point in sCP to the fitted curve is computed and only a second set of points p_2 with distances $< 5\,mm$ are retained. Following each iteration, if the size of the sets $(p_1 + p_2) > 40\%$ of the total points (i.e. sCP) then the combined set of points in p_1 and p_2 are recorded for comparison with the next iteration, and the average curvature value of these points is computed. If the size of the sets $(p_1 + p_2) \leq 40\%$ of the total points (i.e. sCP) then the combined set of points in p_1 and p_2 are not considered for comparison with the next iteration. Currently, this process is iterated for a maximum of 100 iterations (future work will incorporate iterations until all the points in sCP have been sampled), and the retained set of points with the minimum average curvature value is identified as the set of detected breast contour points, and the resulting fitted cubic spline curve is identified as the breast contour.

2.4. Evaluation metric

We use a similarity measure called dice coefficient [17] to evaluate the results of our algorithm for detecting the 3D breast contour. We compute the dice coefficient between automatically detected breast contour using our proposed method and manually selected contour as follows. Since the two contours are not same in length, we keep the same length for comparison based on the shorter one. We interpolate the same number of points from the automatically detected contour points and manually selected contour points using cubic spline method to obtain the interpolated point sets d and m, respectively. For each point in d (or m), we compute the distance to the fitted cubic spline curve from point set m (or d). Let num be the total number of the points in d and m with distances less than a given threshold, the dice coefficient is computed as num over the sum of the total number of points in d and m. The dice coefficient is always in [0, 1] range. A dice coefficient of 1 indicates high

similarity (all points in d and m fall in the distance threshold), whereas 0 indicates little to no similarity (all points in d and m fall out the distance threshold).

3. Data Acquisition

Female patients about to undergo mastectomy and breast reconstruction surgery at The University of Texas MD Anderson Cancer Center were recruited under a protocol approved by the institutional review board. Surface scans were obtained using the 3dMDTorso system (3dMD LLC, Atlanta, GA). Surface images from five patients were used in this study. Age, body mass index (BMI), breast ptosis degree, and pre- and/or post-operative information for the five patients are listed in Table 1. All patients were White with ethnicity of non-hispanic origin.

Table 1. Demographic information for the patients in this study

Patient ID	Age	BMI	Right breast ptosis degree	Left breast ptosis degree
1	57	29.0	1 (pre-operative)	1 (pre-operative)
2	55	22.4	1 (pre-operative)	1 (pre-operative)
3	54	25.9	2 (pre-operative)	2 (pre-operative)
4	46	34.4	2 (pre-operative)	2 (pre-operative)
5	47	27.3	2 (pre-operative)	3 (post-operative)

4. Results

We validated our proposed algorithm using the surface scans for five patients. Data for a representative image is presented in Fig. 4. We show the result on the upper half of the torso (above the umbilicus to sternal notch, Fig. 4A). In Fig. 4B, a color ramp is used to display the Gaussian curvature, ranging from blue to red for increasing curvature values. As seen in Fig. 4C, the set of points sCP includes not only the points lying along the breast contour, but also randomly scattered points on the torso (noise). Results of the proposed algorithm are presented in Fig. 4D. Blue points are manually selected contour points, which are used as ground truth for comparison. Green points are contour points detected using our proposed algorithm. The red curve is obtained via cubic spline fitting of the detected contour points in green. As seen in Fig 4D, high correspondence is achieved between the manually selected points and the automatically detected breast contour.

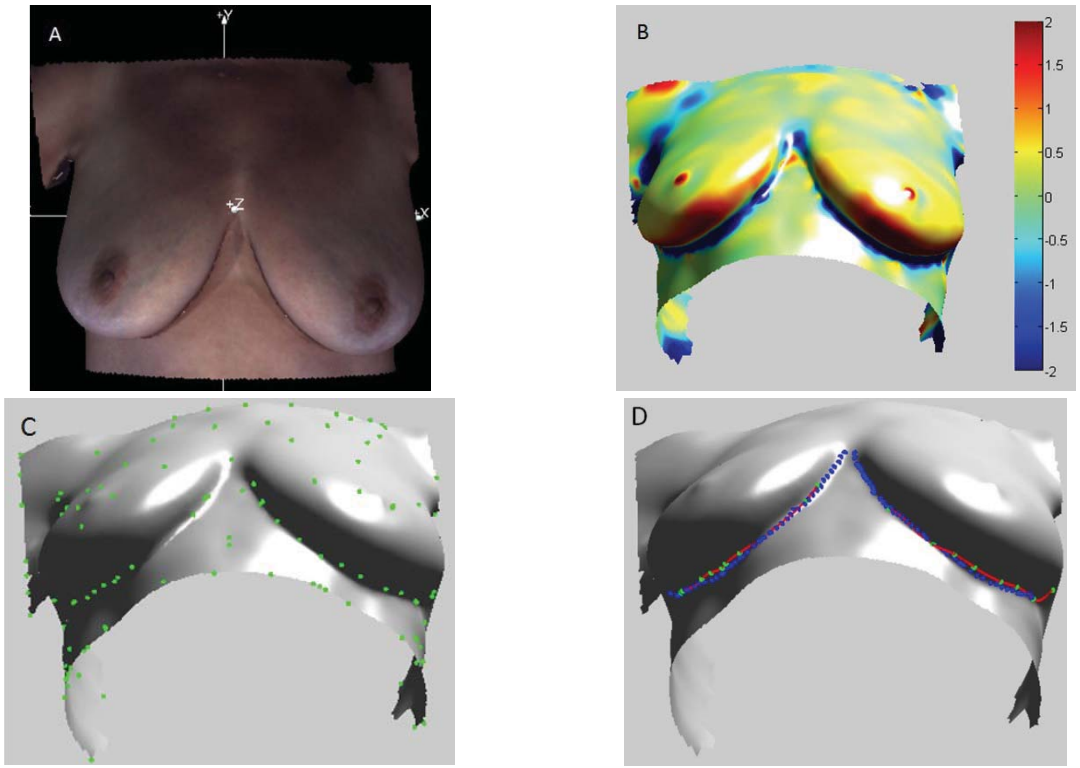

Fig. 4. (A) 3D Surface scan, (B) Color mapped Gaussian Curvatures of Surface scan, (C) Set of points sCP exhibiting low curvature values displayed on surface (green), (D) Detected contour (red) and manually selected

contour points (blue) displayed on surface.

Table 2 presents the dice coefficients for automated versus manually selected breast contours for five patients. The distance threshold represents the separation between the points on the two contours. We tested dice coefficients using 6 thresholds: $0.5\,mm$, $1.0\,mm$, $2.0\,mm$, $3.0\,mm$, $4.0\,mm$, and $5.0\,mm$. The average dice coefficient is the average value for the 10 breasts of the 5 patients at a given distance threshold. From Table 2 we can see that as the distance threshold for similarity between two contours is increased, the dice coefficient also increases. At a separation distance in the range of $3\,mm - 5\,mm$ between the automatically detected and manually annotated breast contours, we have very high dice coefficient values (0.94−0.97). At a resolution of $2\,mm$ the similarity is around 0.8 (80%), and is reduced only for very low threshold values of $1\,mm$ (55%), and $0.5\,mm$ (28%).

Table 2. Dice coefficient for automatically detected versus manually selected breast contours (BC)

Patient ID	Dice Coefficient											
	Distance threshold (0.5mm)		Distance threshold (1.0mm)		Distance threshold (2.0mm)		Distance threshold (3.0mm)		Distance threshold (4.0mm)		Distance threshold (5.0mm)	
	Right BC	Left BC	Right BC	Left BC	Right BC	Left BC	Right BC	Left BC	Right BC	Left BC	Right BC	Left BC
1	0.57	0.33	0.975	0.655	0.995	1	1	1	1	1	1	1
2	0.22	0.11	0.465	0.255	0.935	0.545	0.995	0.93	1	0.955	1	0.965
3	0.02	0.19	0.215	0.36	0.465	0.615	0.665	0.845	0.8	0.885	0.88	0.905
4	0.46	0.10	0.705	0.25	0.975	0.575	0.985	0.95	0.995	0.995	1	1
5	0.44	0.35	0.79	0.825	0.96	1	0.965	1	0.965	1	0.965	1
Average	0.28		0.55		0.81		0.94		0.96		0.97	

5. Conclusions

We have developed a Gaussian curvature-based automated breast contour detection algorithm for 3D images of the female torso. Our approach employs the RANSAC algorithm to accurately obtain the lower breast contour, as compared to the manually selected contour. For a $2.0\,mm$ distance threshold between the manual and automatically detected contour, the dice coefficient is 0.81; and for a distance threshold of $3.0\,mm$, the dice coefficient is 0.94. Based on our experimental results, the proposed algorithm can successfully detect the lower contours for breasts with ptosis degrees in the range of 1 - 3. However, more experiments are required to improve our method and to demonstrate the significance of our results. Currently, the proposed method can only detect the lower part of the breast contour. Future work will also extend the algorithm design to include the identification of the upper pole breast contour, in order to enable measurement of the closed breast foot-print on the chest wall. The ability to visualize and quantify morphological features of the breast facilitates pre-operative planning and post-operative outcome assessment.

Acknowledgements

This work was supported by a NIH grant 1R01CA143190-01A1. The patient data used in this study were generously provided by Mark Villa, M.D., David Chang, M.D., Charles Butler, M.D., Patrick Garvey, M.D., and Geoffrey Robb, M.D., of the Department of Plastic Surgery at The University of Texas MD Anderson Cancer Center.

References

1. Bostwick, J. I., (1999): “Plastic and reconstructive breast surgery”, 2nd Ed., St. Louis, Missouri: Quality Medical Publishing, Inc.
2. Eric, M., Mihic, N., and Krivokuca, D., (2009): “Breast reconstruction following mastectomy; patient's satisfaction”, Acta Chirurgica Belgica, Vol. 109, No. 2, pp. 159-166.
3. Losken, A., Fishman, I., Denson, D. D., Moyer, H. R., and Carlson, G. W., (2005): “An objective evaluation of breast symmetry and shape differences using 3-dimensional images”, Annals of Plastic Surgery , Vol. 55, No. 6, pp. 571-575.
4. Kovacs, L., Eder, M., Hollweck, R., Zimmermann, A., Settles, M., Schneider, A., Endlich, M., Mueller, A., Schwenzer-Zimmerer, K., Papadopulos, N. A., and Biemer, E., (2007): “Comparison

between breast volume measurement using 3D surface imaging and classical techniques", Breast Vol. 16, pp. 137-45.
5. Losken, A., Seify, H., Denson, D. D., Paredes, A. A. Jr., and Carlson, G. W., (2005): "Validating three-dimensional imaging of the breast", Annals of Plastic Surgery, Vol. 54, No. 5, pp. 471-476, discussion 477-478.
6. Cardoso, J. S., Teixeira, L. F., and Cardoso, M. J., (2008): "Automatic Breast Contour Detection in Digital Photographs", Proceedings of International Conference on Health Informatics (HEALTHINF 2008), Funchal, Madeira, Portugal, Vol. 2, pp. 91-98.
7. Cardoso, J. S., Sousa, R., Teixeira, L. F., and Cardoso, M. J., (2008): "Breast contour detection with stable paths", Biomedical Engineering Systems and Technologies, International Joint Conference, Funchal, Madeira, Portugal, Vol. 25, pp. 439-452.
8. Oliveira, H.P., Cardoso, J.S., Magalhães A., and Cardoso M.J., (2012): "Depth-Map Images for the Aesthetic Evaluation of Breast Cancer Treatment", Proceedings of the 1st PhD. Students Conference in Electrical and Computer Engineering, Porto, Portugal, pp. 1-2.
9. Oliveira, H. P., Cardoso, J. S., Magalhães, T., and Cardoso, J. S., (2012): "Simultaneous Detection of Prominent Points on Breast Cancer Conservative Treatment Images", 19th IEEE International Conference on Image Processing, Orlando, Florida, pp. 2841-2844.
10. Lee, J., Chen, S., Reece, G. P., Crosby, M. A., Beahm, E. K., and Markey, M. K., (2012): "A novel quantitative measure of breast curvature based on catenary", IEEE Transactions on Biomedical Engineering, Vol. 59, No. 4, pp. 1115-1124.
11. Lee, J., Muralidhar, G. S., Reece, G. P., and Markey, M. K., (2012): "A Shape Constrained Parametric Active Contour Model for Breast Contour Detection", Engineering in Medicine and Biology Society, Proceedings of the 34th Annual International Conference of the IEEE, San Diego, California, pp. 4450-4453.
12. Lee, J., Reece, G. P., and Markey, M. K., (2012): "Breast curvature of the upper and lower breast mound: 3D analysis of patients who underwent breast reconstruction", 3rd International Conference on 3D Body Scanning Technologies, Lugano, Switzerland, pp. 171-179.
13. Gabriel Peyre, Toolbox Graph, (accessed 2013): http://www.mathworks.com/matlabcentral/fileexchange/5355-toolbox-graph.
14. Cohen-Steiner, D., and Jean-Marie, M., (2003): "Restricted delaunay triangulations and normal cycle", Proceedings of the nineteenth Conference on Computational Geometry (SCG-03), New York, pp. 237-246.
15. Alliez, P., Cohen-Steiner, D., Desburn, M., Devillers, O., and L´evy, B., (2003): "Anisotropic polygonal remeshing", SIGGRAPH 2003, Vol. 22, No. 3, pp.485-493.
16. Fischler, M. A., and Bolles, R. C., (1981): "Random Sample Consensus: A Paradigm for Model Fitting with Applications to Image Analysis and Automated Cartography", Communications of the ACM, Vol. 24, pp. 381-395.
17. Murguía, M., and Villaseñor, J. L., (2003): "Estimating the effect of the similarity coefficient and the cluster algorithm on biogeographic classifications", Annales Botanici Fennici, Vol. 40, No. 6, pp. 415-421.